International Journal of Chronic Obstructive Pulmonary Disease Dovepress
open access to scientific and medical research

Open Access Full Text Article

ORIGINAL RESEARCH

Network Pharmacology Followed by Experimental Validation to Explore the Mechanism of Stigmasterol in Sangbaipi Decoction Regulating PI3K/Akt Signaling to Alleviate Acute Exacerbation of Chronic Obstructive Pulmonary Disease

Haidong He[1], Shuihua Sun[2], Weihua Xu[1], Mingwan Zhang[3]

[1]Department of Pulmonary and Critical Care Medicine, Tongde Hospital of Zhejiang Province, Hangzhou City, Zhejiang Province, People's Republic of China; [2]Department of Medical Oncology, Tongde Hospital of Zhejiang Province, Hangzhou City, Zhejiang Province, People's Republic of China; [3]Department of Pharmacy, Tongde Hospital of Zhejiang Province, Hangzhou City, Zhejiang Province, People's Republic of China

Correspondence: Haidong He, Department of Pulmonary and Critical Care Medicine, Tongde Hospital of Zhejiang Province, 234 Gucui Road, Cuiyuan Street, Xihu District, Hangzhou City, Zhejiang Province, 310012, People's Republic of China, Tel +86-571-89972427, Email hhd0901190040@163.com

Purpose: Sangbaipi decoction (SBPD), a traditional Chinese medicine (TCM) prescription, has been widely used to treat acute exacerbation of chronic obstructive pulmonary disease (AECOPD), while the underlying pharmacological mechanism remains unclear due to the complexity of composition.

Methods: A TCM-active ingredient-drug target network of SBPD was constructed utilizing the TCM-Systems-Pharmacology database. AECOPD-relevant proteins were gathered from Gene Cards and the Online-Mendelian-Inheritance-in-Man database. Protein–protein interaction, GO and KEGG enrichment analyses of the targets from the intersection of SBPD and AECOPD targets were performed to identify the core signaling pathway, followed by molecular docking verification of its interaction with active ingredients. The network pharmacology results were checked using *in-vivo* experiments. To induce AECOPD, rats were exposure to combined tobacco smoke and lipopolysaccharide (LPS). Then rats underwent gavage with stigmasterol (SM) after successful modeling. The involvement of phosphoinositide 3-kinase (PI3K)/protein kinase B (Akt) signaling was investigated using its inhibitor, LY294002. Lung function and histopathology were examined. The levels of inflammatory cytokines in the lung and serum were assessed by quantitative reverse transcription-polymerase chain reaction (qRT-PCR), Western blot and/or Enzyme-linked immunosorbent assay (ELISA).

Results: SM was recognized as an active ingredient of SBPD and stably bound to Akt1. SM improved lung function and histological abnormalities, concomitant with suppressed PI3K/Akt signaling, downregulated lung and serum Interleukin 6 (IL-6) and tumor necrosis factor-α (TNF-α) levels and serum transforming growth factor-β (TGF-β) levels and upregulated lung and serum Interleukin 10 (IL-10) levels in AECOPD rats. In AECOPD rats, LY294002 restored lung function, and it also improved lung histological abnormalities and inflammation, which was found to be potentiated by SM.

Conclusion: SM targets PI3K/Akt signaling to reduce lung injury and inflammation in AECOPD rats.

Keywords: sangbaipi decoction, stigmasterol, acute exacerbation of chronic obstructive pulmonary disease, PI3K/Akt signaling, lung inflammation

Introduction

Chronic obstructive pulmonary disease (COPD) is a common preventable and treatable condition characterized by persistent airflow limitation, which is often progressive and associated with a promoted chronic inflammatory response of the airways and lungs to toxic particles or gases.[1] Treatments ranging from pharmacotherapy to bronchoscopic and surgical interventions render COPD patients with decreased morbidity and mortality.[2,3] Nonetheless, patients may

Received: 16 January 2024
Accepted: 22 July 2024
Published: 8 August 2024

experience worsening of respiratory symptom upon acute viral/bacterial infections, incurring acute exacerbations of COPD (AECOPD).[4,5]

AECOPD has major adverse consequences to patients and health care system, and represents the most considerable proportion of socioeconomic burden of COPD.[6] It is characterized by potentiated airway inflammation, mucus hypersecretion and marked gas trapping, resulting in accelerated lung function decline, impaired quality-of-life and increased mortality.[4,6] Current management of AECOPD, mainly resorts to the use of bronchodilators and systemic steroids and antibiotics,[7] which unfortunately can cause adverse effects and show limited efficacy due to drug resistance.[8] Further, disease recurrence is common and detrimental to patients' outcome, as it increases the risk of entering a cycle of frequent exacerbations that trigger further decline.[6] In this case, novel treatments with higher efficacy and less side effects are in dire need of being proposed.

Traditional Chinese medicine (TCM) prescriptions, which have been collected in ancient medical books, have been used as drugs or health dietary supplements in China for hundreds of years and with the advantages of high safety, and good clinical efficacy.[9,10] TCM can safely and effectively improve menopause-like syndrome in breast cancer, treat allergic, cardiovascular, chronic liver diseases, etc.[11–14] TCM contains a large number of flavonoids, alkaloids, terpenoids, polyphenols and other effective anti-lung cancer active compounds, which are suitable as candidate drugs for the treatment of lung cancer.[15] Previous study showed that Qiju granules effectively protect lung function from the adverse effects of PM2.5 exposure.[16] The application of TCM prescriptions to the treatment of AECOPD with inflammation as the main therapeutic target has exhibited significant effect in restoring lung function.[17,18] Sangbaipi decoction (SBPD) is a Ming dynasty-generated TCM prescription that have been extensively applied clinically in China along with Western medicines to the treatment of AECOPD and results in improved clinical efficacy.[19] It is composed of diverse TCMs including Mori Cortex, Scutellaria Baicalensis, Arum Ternatum Thunb, Coptidis Rhizoma, Perillae Fructus, Rhizoma Zingiberis Recens, Gardeniae Fructus, Fritillaria Cirrhosa, Amygdalus Communis Vas.[20] Systematic review and meta-analysis of the effect of SBPD on AECOPD have demonstrated heat-clearing, phlegm-reducing anti-inflammatory and immunomodulating activities conferred by SBPD and attributed these effects to the TCMs SBPD comprises.[20] However, due to the complexity of SBPD's composition, the molecular mechanism of its action has yet to be unveiled, limiting its application and promotion in clinical practice to some extent.

Recent years have witnessed a continually declining rate of the success of drug discovery, which is in part due to the "one disease-one target-one drug" dogma.[21] Considering the complexity of SBPD's composition, this dogma may obstruct the molecular mechanism of its action from being fully clarified. Network pharmacology is an emerging discipline that integrates the technologies and contents of multiple disciplines such as pharmacology, systems biology, and computational biology. It utilizes a large number of network database resources to predict the targets of drug, thereby constructing a multi-level drug-composition-target-disease interaction network to explain the mechanism underlying a multi-pathway and multi-target treatment method from the perspective of micro-pharmacological regulation of gene expression.[21,22]

In this present study, the main active ingredients, targets and signaling pathways by which SBPD exerts therapeutic effect on AECOPD were explored based on network pharmacology, subsequent to which the binding ability of the obtained active ingredient to the obtained targets was verified using molecular docking simulation and the involvement of the core signaling pathway obtained, namely phosphoinositide 3-kinase (PI3K)/protein kinase B (Akt) signaling was investigated using animal experiments, so as to provide a theoretical basis for the clinical application of SBPD in the treatment of AECOPD.

Materials and Methods

Bioinformatics Analyses

Screening of Active Ingredients and Targets of TCMs

The active ingredients of Mori Cortex (its name in Chinese phonetic alphabets (NCPA): Sangbaipi; Voucher Number: 0005225; Herbarium: College of Pharmacy, Guiyang University of TCM; Identification: Yuan Gui Huang), Scutellaria Baicalensis (NCPA: Huangqin; Voucher Number: 02099364; Herbarium: Institute of Botany, Academia Sinica; Identification: Gen Sheng Zhou), Arum Ternatum Thunb (NCPA: Banxia; Voucher Number: 02240647; Herbarium:

Institute of Botany, Academia Sinica; Identification: Qi Lin), Coptidis Rhizoma (NCPA: Huanglian; Voucher Number: 01962061; Herbarium: Institute of Botany, Academia Sinica; Identification: Wencai Wang), Perillae Fructus (NCPA: Zisuzi; Voucher Number: 02010112; Herbarium: Institute of Botany, Academia Sinica; Identification: Qiang Wang), Rhizoma Zingiberis Recens (NCPA: Shengjiang; Voucher Number: 1268515; Herbarium: Kunming Institute of Botany, Chinese Academy of Sciences; Identification: Guoda Tao), Gardeniae Fructus (NCPA: Zhizi; Voucher Number: 0400111; Herbarium: South China Botanical Garden, Chinese Academy of Sciences; Identification: Liangzhi Jia), Fritillaria Cirrhosa (NCPA: Chuanbeimu; Voucher Number: 01859273; Herbarium: Institute of Botany, Academia Sinica; Identification: Xinqi Chen), and Amygdalus Communis Vas (NCPA: Kuxingren; Voucher Number: 0015751; Herbarium: College of Pharmacy, Guiyang University of TCM; Identification: Lianjun Guo) were screened out through the Traditional Chinese Medicine Systems Pharmacology database (TCMSP; http://tcmspw.com), with a filter conditioned at the bioavailability (OB) ≥30% and the druglikeness (DL) ≥ 0.18. The obtained main active ingredients were imported into TCMSP to retrieve the corresponding targets. Meanwhile, UniProt (https://www.uniprot.org) was used with the species defined as homo sapiens, to calibrate the genetic information of the targets, and thus to obtain the standardized name of the targets. All plant material sampled for research in this experiment required no permissions.

Construction of "TCM-Active Ingredient-Drug Target" Networks

Based on the obtained active ingredients and target genes, by running a plug-in, Network Analyzer for topological analysis, a "TCM-active ingredient-target gene" network was plotted on Cytoscape 3.7.2 (https://cytoscape.org). The core constitutes were screened out according to the degree value.

Screening of Disease-Relevant Targets

Gene Cards (https://www.genecards.org) and the Online Mendelian Inheritance in Man database (OMIM; http://www.omim.org) were utilized to search for target genes with "acute exacerbation of chronic obstructive pulmonary disease" as a search term, and target genes were finally obtained by combining and removing duplicate values.

Screening of Drug-Disease Shared Targets

The targets of SBPD and the AECOPD-relevant targets were introduced into Venny 2.1.0 online software (https://bioinfogp.cnb.csic.es/tools/venny) for intersection analysis, where a Venny diagram was plotted to yield targets shared by SBPD and AECOPD.

Construction of Protein–Protein Interaction (PPI) Networks

The SBPD-AECOPD shared targets were imported upon STRING (http://cn.string-db.org), with the species defined as homo sapiens and the confidence level set at ≥0.4 eliminating three non-interacting targets, to output a PPI network. The related TSV format file was then obtained. That file was further imported into Cytoscape 3.7.2, demonstrating the PPI network including 202 nodes and 4313 edges. After running with its plug-in CytoNCA for topological analysis, the Top 10 core target genes of PPI network were screened out according to the degree value.

Pathway and Functional Enrichment Analysis

The SBPD-AECOPD shared targets were input into Metascape (https://metascape.org), and the biological species was set as homo sapiens. Subsequently, Gene Ontology (GO) and Kyoto Encyclopedia of Genes and Genomes (KEGG) enrichment pathway analysis were performed according to P <0.01, and R language was utilized for visualization.

Molecular Docking Verification

The core targets were obtained through screening the core PPI network, and then their corresponding active ingredients were determined. A molecular docking software, AutoDock Vina 1.1.2 (https://github.com/ccsb-scripps/AutoDock-Vina/releases), was used to verify the reliability of the predicted active ingredients and core targets of SBPD. Briefly, the 2D structures of the core active ingredients were obtained from PubChem (https://pubchem.ncbi.nlm.nih.gov) and optimized using Chem3D to generate their 3D structures. Moreover, hydrogenation, charge distribution, and the addition of rotational flex keys were realized with AutoDock 4.2.6 (http://autodock.scripps.edu/), and the results were saved as a "pdbqt": file. PDB was used to search for the 3D structures of the target proteins, which later uploaded

into PYMOL 2.3.0 (https://github.com/schrodinger/pymol-open-source) to removing their water molecules and ligands. AutoDock 4.2.6 was again used for hydrogenation and charge distribution and the related "pdbqt" file was saved. Ultimately, the binding energy was calculated through performing molecular docking of the receptor proteins and ligand small molecules by using AutoDock Vina 1.1.2, with a lower the binding energy indicating a stronger binding stability and the binding energy ≤-5.0 kJ/mol as the standard of a stable binding. Visualization was realized with PYMOL2.3.0.

Ethics Statement

All animal experiments were performed under a project license issued by the Ethics Committee of Zhejiang Academy of Traditional Chinese Medicine (approval number: KTSC2022220) according to the guidelines of the National Institutes of Health on Animal Care and Use.

AECOPD Establishment, Stigmasterol (SM) Gavage and LY294002 Injection

Male Sprague-Dawley rats (n=120), weighing 250–350 g, were maintained in a temperature-controlled room (21± 2.0°C) at a 55 ± 15% humidity on a 12 h/12 h light/dark circadian cycle, and allowed standard rodent house chow diet and water *ad libitum*.

For evaluating the therapeutic effect of SM on AECOPD-associated lung injury, rats were randomly divided into three groups, Control, Model, and Model+SM groups (n=15/group), and further to decipher the mechanism underlying that impact of SM, Control, Model, Model+SM, Model+LY294002 and Model+SM+LY294002 groups were set with 15 rats randomly assigned in each group.

After a 7-day accommodation to the facility, AECOPD was induced in the groups involving modeling by combined administration of lipopolysaccharide (LPS; 437620, Sigma-Aldrich, St. Louis, MO, USA) and tobacco smoke (TS; generated from the combustion of 20 1R3F cigarettes, Kentucky Tobacco Research & Development Center, Orlando, FL, USA). AECOPD was performed based on reference,[23] in brief, the rats underwent exposure to TS for 30 min twice daily, with an interval of at least 5 h between each exposure. On the morning of the 7, 14, 21 day, aerosolized LPS (1 mg/kg) generated by an ultrasonic nebulizer (ATM 210, Topas, Dresden, Germany) was employed to stimulate the rats for 30 min (the injection of LPS is not smoked on the same day). In the Control group, the same protocol was followed, but instead of TS and aerosolized LPS, rats underwent exposure to room air for 30 min in the place of each TS exposure, and were exposed for 30 min to a saline aerosol generated in the same manner as the aerosolized LPS was generated, when LPS exposure should have happened. SM (700062P, $C_{29}H_{48}O$, purity: >99%, 200 mg/kg,[24] Sigma-Aldrich, USA) or its vehicle (sterile water) was taken by the rats of the treatment-related groups via gavage for 14 days after successful modeling.

After all the exposure protocols were completed, the rats in the intervention groups, namely the Model+LY294002 and Model+SM+LY294002 groups were intraperitoneally injected with an inhibitor of PI3K/Akt, LY294002 (HY-10108, MedChemExpress, Monmouth Junction, NJ, USA), at a dose of 100 μM/kg, once a day.[25] On the fourth day, all the rats were anaesthetized via inhalation of 5% isoflurane (PHR2874, Sigma-Aldrich, USA), and received lung function assessment and collected the blood. Finally, rats were conducted euthanasia through cervical dislocation under anesthesia via intraperitoneal injection of pentobarbital sodium (P010, 45 mg/kg, Sigma-Aldrich, USA). Lung tissues were then collected.

Lung Function Assessment

After rats were anaesthetized, a small transverse incision made in the neck in order to expose the trachea and then insert a tracheal intubation tube. The tracheal cannula was further connected to an eSpira Forced Manoeuvers system (TODAY'S EQUIPMENT, Hanoi, Vietnam) to measure the total lung capacity, forced vital capacity, peak inspiratory flow (PIF) and peak expiratory flow (PEF) of rats.

Histopathological Examination

Rat lung tissues were fixed by 4% paraformaldehyde (P885233, MACKLIN, Shanghai, China) for 48 h, dehydrated in gradient ethanol for 5 h, transparentized using xylene (95682, Sigma-Aldrich, USA), and paraffinized (1496904, Sigma-Aldrich, USA), after which the tissues were sectioned to be 4-μm thick slices. The slices underwent routine dewaxation and rehydration, followed by being stained with hematoxylin (HY-N0116, MedChemExpress, USA) for 10 min. Later, the slices were differentiated by 1% hydrochloric ethanol and immersed in weakly alkaline water (67362, Sigma-Aldrich, USA) to develop blue. Sequentially, eosin (HY-D0505A, MedChemExpress, USA) was used to stain the slices for 5 min. Thereafter, slice dehydration and hyalinization were performed before sealing with neutral balsam (N861409, Macklin, Shanghai, China). Lung pathological abnormalities were observed by an optical microscope (ZEISS Primotech, Carl Zeiss, Oberkochen, Germany) under magnifications of ×40 and ×100.

Quantitative Reverse Transcription-Polymerase Chain Reaction (qRT-PCR)

Total RNA from rat lung tissues were extracted using Trizol reagent (15596026, ThermoFisher, Waltham, MA, USA), and reverse-transcribed into cDNA by utilizing reverse transcription kits (K1622, Yaanda Biotechnology, Beijing, China). Thereafter, real-time PCR reaction was carried out by using SYBR Green Super Mix kits (1725272, BIO-RAD, Hercules, CA, USA) on a system (LightCycler 96, Roche, Indianapolis, IN, USA). A typical cycling condition was set, including 95°C for 10 min, followed by 40 cycles of 95°C for 10s, 60°C for 30s, and 72°C for 1 min. The primer used are listed in Table 1. Relative expression of genes were calculated using the $2^{-\Delta\Delta Ct}$ method,[26] with β-actin serving as the normalizer.

Western Blot

Total protein from rat lung tissues was isolated using RIPA buffer supplemented with inhibitors of protease and phosphatase (A32961, ThermoFisher, USA). BCA kits (A53227, ThermoFisher, USA) were employed for determination of the protein concentration. The isolated protein (50 μg) was separated by SDS-PAGE gel (1615100, BIO-RAD, USA), and transferred to PVDF membranes (1620256, BIO-RAD, USA), which were later blocked in 5% skimmed milk at room temperature for 2 h. Afterwards, the membranes were incubated with primary antibodies for interleukin-6 (IL-6; ab281935, 23 kDa, 1:1000, Abcam, Cambridge, UK), tumor necrosis factor-α (TNF-α; ab205587, 26 kDa, 1:1000, Abcam, UK), interleukin-10 (IL-10; ab192271, 20 kDa, 0.1 μg/mL, Abcam, UK), PI3K (ab154598, 126 kDa, 1:500, Abcam, UK), phosphorylated (p)-PI3K (ab182651, 84 kDa, 1:200, Abcam, UK), AKT (ab8805, 60 kDa, 1:500, Abcam, UK), phosphorylated (p)-AKT (ab38449, 56 kDa, 1:500, Abcam, UK) and β-actin (ab8226, 42 kDa, 1 μg/mL, Abcam, UK) at 4°C overnight. Following being washed thrice by TBST (37573, ThermoFisher, USA), the membranes were subjected to a 1-h incubation with secondary antibodies (Goat anti-Rabbit/Mouse IgG; ab97051/ab205719, Abcam, UK) at room temperature. The protein bands were scanned on an imaging system (ChemiDoc, BIO-RAD, USA) with ECL substrate (1705060, BIO-RAD, USA), and densitometrically analyzed using Image-Pro Plus 6.0 (Media Cybernetics, Silver Spring, MD, USA).

Enzyme-Linked Immunosorbent Assay (ELISA)

Rat serum was obtained by centrifugation of rat blood at 1000×g for 10 min. The levels of IL-6, TNF-α, IL-10 and transforming growth factor-β (TGF-β) in the serum were detected using ELISA kits (ab100772, ab236712, and

Table 1 Primers Used in Quantitative Reverse Transcription Polymerase Chain Reaction for Related Genes

Genes	Species	Forward (5'- −3')	Reverse (5'- −3')
IL-6	rat	ATCTGCCCTTCAGGAACAGC	CTCAATAGCTCCGCCAGAGG
TNF-α	rat	AGAGCGGTGATTCAAAGGCA	TTCCACGTCCCATTGGCTAC
IL-10	rat	CCGAATGCTTCCCTTTCCCT	CCTTGCACCTTCTCCGACTT
β-actin	rat	TACCCAGGCATTGCTGACAG	TATGGGTCCAGGCTAAGGCT

ab214566, Abcam, UK) and (EK981, MULTI SCIENCE, Hangzhou, China). Simply put, after being diluted, the serum (50 μL) was added into enzyme-coated 96-well plates. The plates were then incubated with 50 μL biotin-labelled Antibody, followed by incubation at 37°C for 1.5 h at room temperature. Later, the plates were reacted with streptavidin-HRP solution for 30 min, after which 100 μL TMB substrate was added for color development. The absorbance at 450 nm was measured by a microplate reader (PHERAstar FSX, BMG LABTECH, Ortenberg, Germany), following the addition of 100 μL stop solution.

Statistical Analysis

Statistical analysis was processed with GraphPad prism (version 8.0, GraphPad Software Inc., San Diego, CA, USA). All data were represented in terms of mean ± standard deviation (SD) from triplicate experiments. One-way analysis of variance (ANOVA) was exploited for comparison. $P < 0.05$ was taken to indicate a statistical significance.

Results

Network Pharmacology-Based Construction of "SBPD-Active Ingredient-Drug Target" Networks and Prediction of the Core Signaling Pathway

Network pharmacology technology was applied to preliminarily excavate the active ingredients, targets and signaling pathways by which SBPD combats AECOPD. Through searching TCMSP for drug targets with OB≥30% and DL≥0.18 as conditional filters and eliminating active ingredients without corresponding targets, we retrieved a total of 112 active ingredients, including 20 kinds of Mori Cortex, 27 kinds of Scutellaria Baicalensis, 8 kinds of *Arum* Ternatum Thunb, 8 kinds of Coptidis Rhizoma, 8 kinds of Perillae Fructus, 2 kinds of Rhizoma Zingiberis Recens, 8 kinds of Gardeniae Fructus, 8 kinds of Fritillaria Cirrhosa, 10 kinds of Amygdalus Communis Vas, and 13 kinds of coactive ingredients (Figure 1). Then, the name of all these targets were calibrated using UniProt. A total of 277 targets were obtained by removing the duplicate and invalid values (Figure 1). For the convenience of subsequent

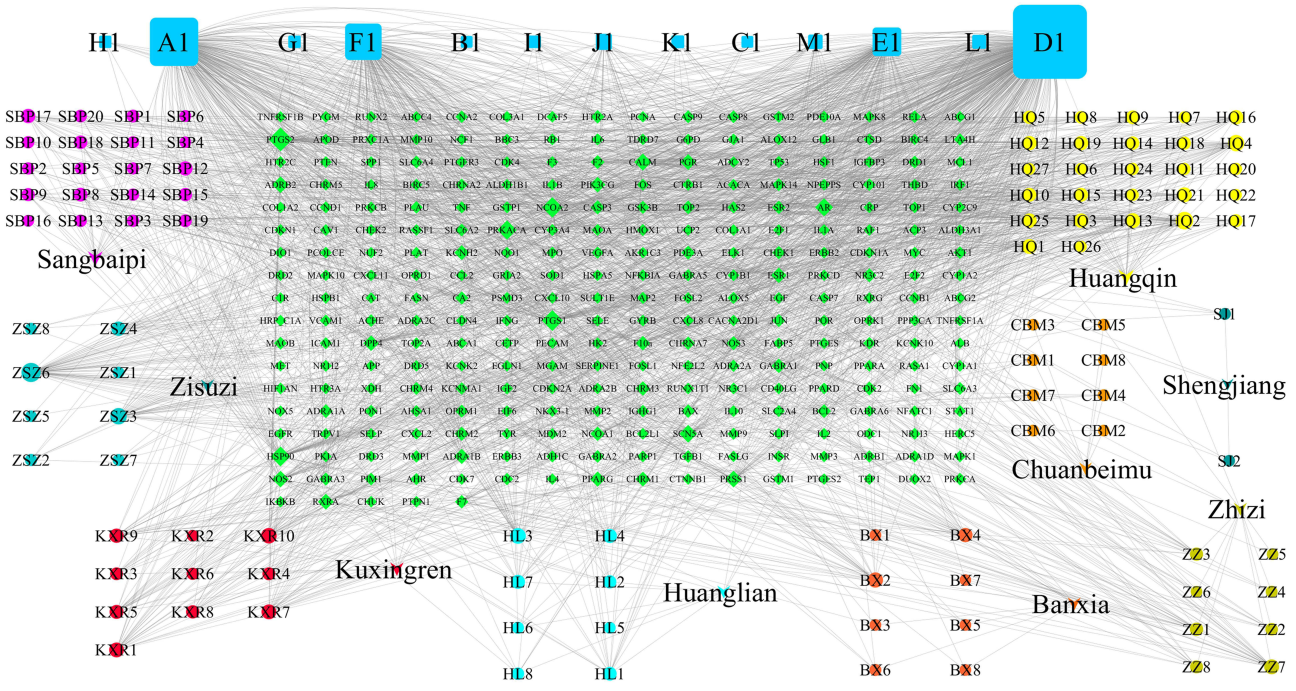

Figure 1 Network pharmacology-based construction of "TCM-Active Ingredient-Drug Target" networks. The TCM-active ingredient-drug target network of SBPD was constructed using the Traditional Chinese Medicine Systems Pharmacology database combined with Cytoscape 3.7.2 plugged with Network Analyzer.

Abbreviations: SBPD/SBP Decoction, Sangbaipi decoction; TCM, traditional Chinese medicine; AECOPD, acute exacerbation of chronic obstructive pulmonary disease; Sangbaipi, Mori Cortex; Huangqin, Scutellaria Baicalensis; Banxia, Arum Ternatum Thunb; Huanglian, Coptidis Rhizoma; Zisuzi, Perillae Fructus; Shengjiang, Rhizoma Zingiberis Recens; Zhizi, Gardeniae Fructus; Chuanbeimu, Fritillaria Cirrhosa; Kuxingren, Amygdalus Communis Vas.

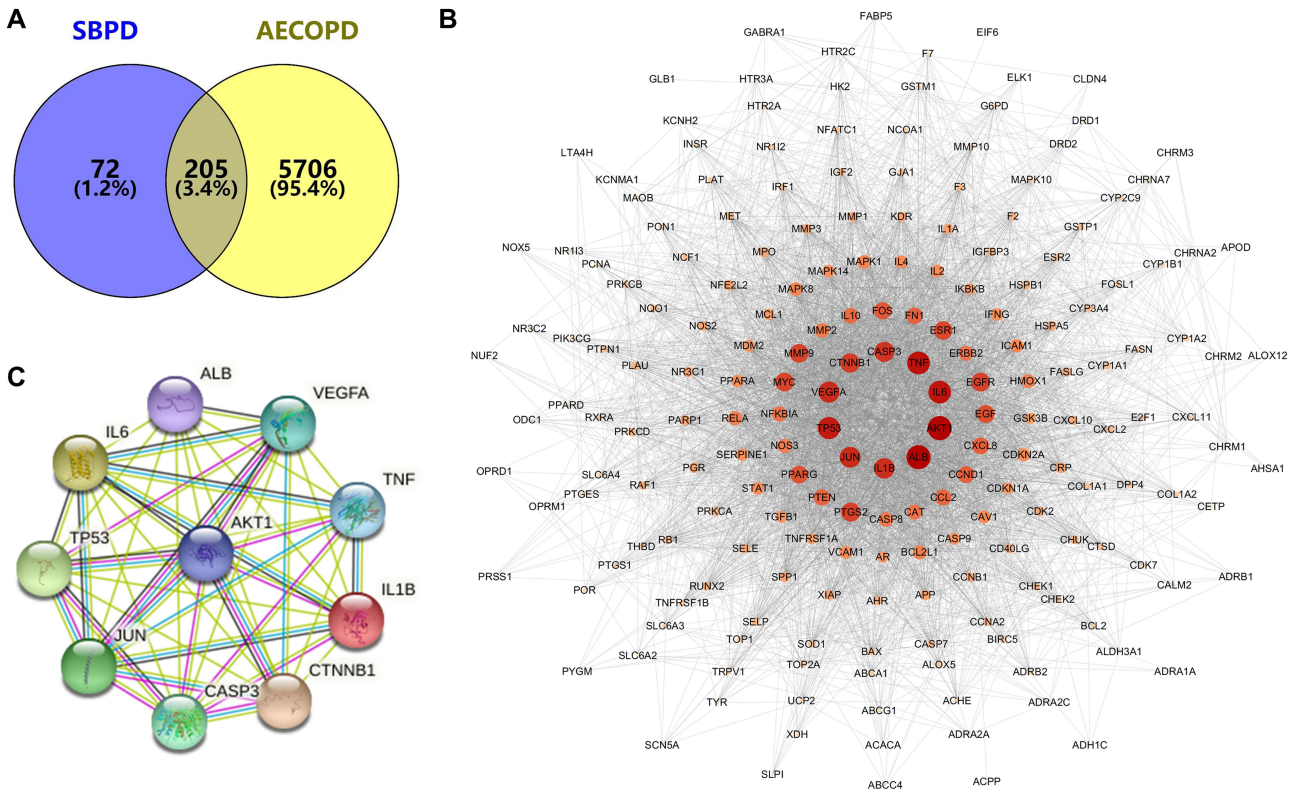

Figure 2 AECOPD target collection and construction of PPI network. (**A**). Gene Cards and the Online Mendelian Inheritance in Man database were used to predict AECOPD-relevant genes, which were intersected with genes targeted by SBPD using a Venny 2.1.0 software. (**B**). The obtained intersection gene targets were imported into STRING to generate a protein-protein interaction network. (**C**). The top 10 core target-constituted protein–protein interaction network.
Abbreviations: SBPD, Sangbaipi decoction; AECOPD, acute exacerbation of chronic obstructive pulmonary disease; PPI, protein–protein interaction; AKT1, protein kinase B 1.

studies, the drugs were coded by the acronym of their NCPAs and those 13 kinds of coactive ingredients were labeled as A1-M1 (Figure 1).

Gene Cards and OMIM were then used to identify the targets of AECOPD. The targets retrieved from these two databases were combined, followed by removing the duplicate values, which gave rise to 5911 targets (Figure 2A). These AECOPD-relevant targets were further intersected with those 277 targets of SBPD, leading to 205 targets, as shown in Figure 2A. Later, the targets from the intersection were imported into STRING for analysis of PPI networks with a confidence level of ≥0.4. As presented in Figure 2B, a PPI network was obtained. It was further uploaded into Cytoscape 3.7.2, which then performed topological analysis using CytoNCA. The obtained target genes were sorted according to their degree value to generate the Top 10 core target genes (Figure 2C). Sequentially, Metascape was employed with $P < 0.01$ as a conditional filter for GO enrichment analysis to identify Biological process (BP), cellular components (CC) and molecular function (MF) mediated by these 10 target genes, and the top 10 items retrieved from the results were displayed in Figure 3A. Afterwards, KEGG enrichment analysis was performed with these target genes with the same parameters, and in the light of their −lgP values, the Top 10 items were yielded, as shown in Figure 3B, which recognizes PI3K/Akt as the key signaling pathway by regulating which SBPD exerts its therapeutic effect on AECOPD.

Molecular Docking of Active Ingredients and Core Protein Targets

AutoDock Vina 1.1.2 was utilized to perform molecular docking simulation between the key target genes and the active ingredients (Figure 4). As illustrated in Table 2, the minimum binding energy value for the docking between the targets and the active ingredients (A, Quercetin-ALB; B, Kaempferol-IL-6; C, Quercetin-Akt1; D, Luteolin-ALB; E, SM-Akt1; F, Kaempferol-Akt1) were all less than −5.0 kJ/mol, suggesting these active ingredients possess a good binding activity

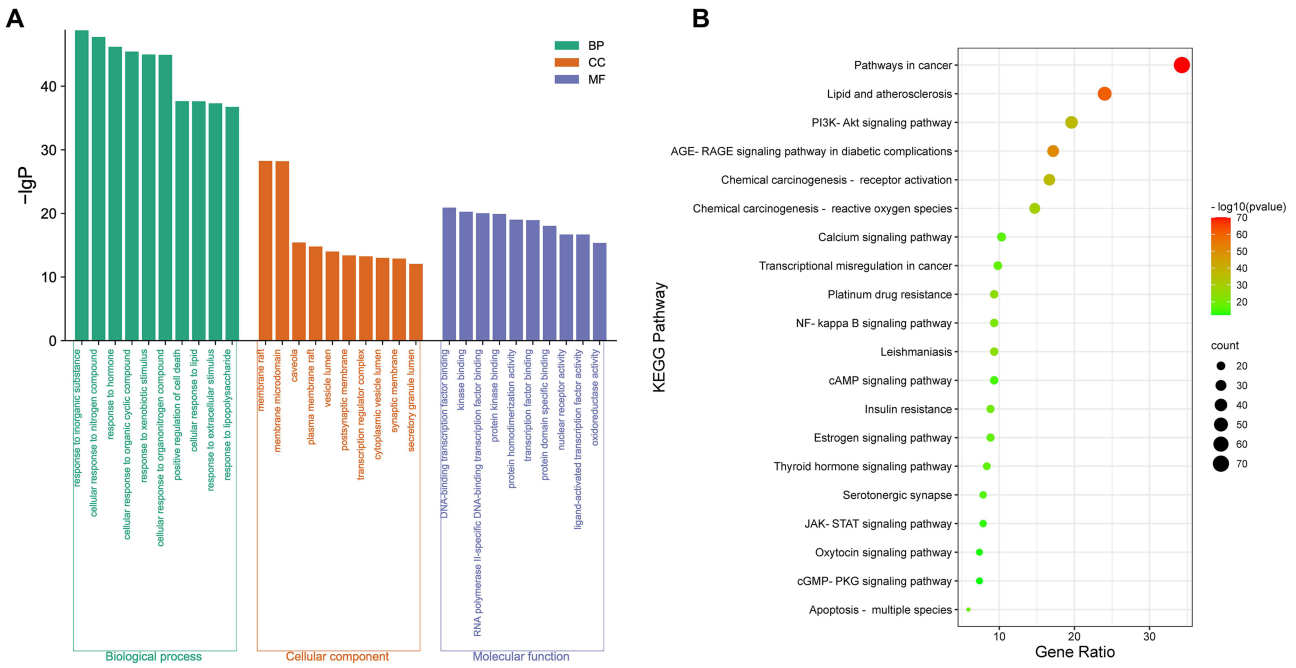

Figure 3 GO function and KEGG pathway enrichment analysis. (**A**). The biological process, molecular function and cellular components controlled by the intersection gene targets were predicted by Gene Ontology enrichment analysis performed in Metascape. (**B**). Kyoto Encyclopedia of Genes and Genomes enrichment analysis performed in Metascape was used to screen out the core signaling pathway.
Abbreviations: BP, biological process; MF, molecular function; CC, cellular components.

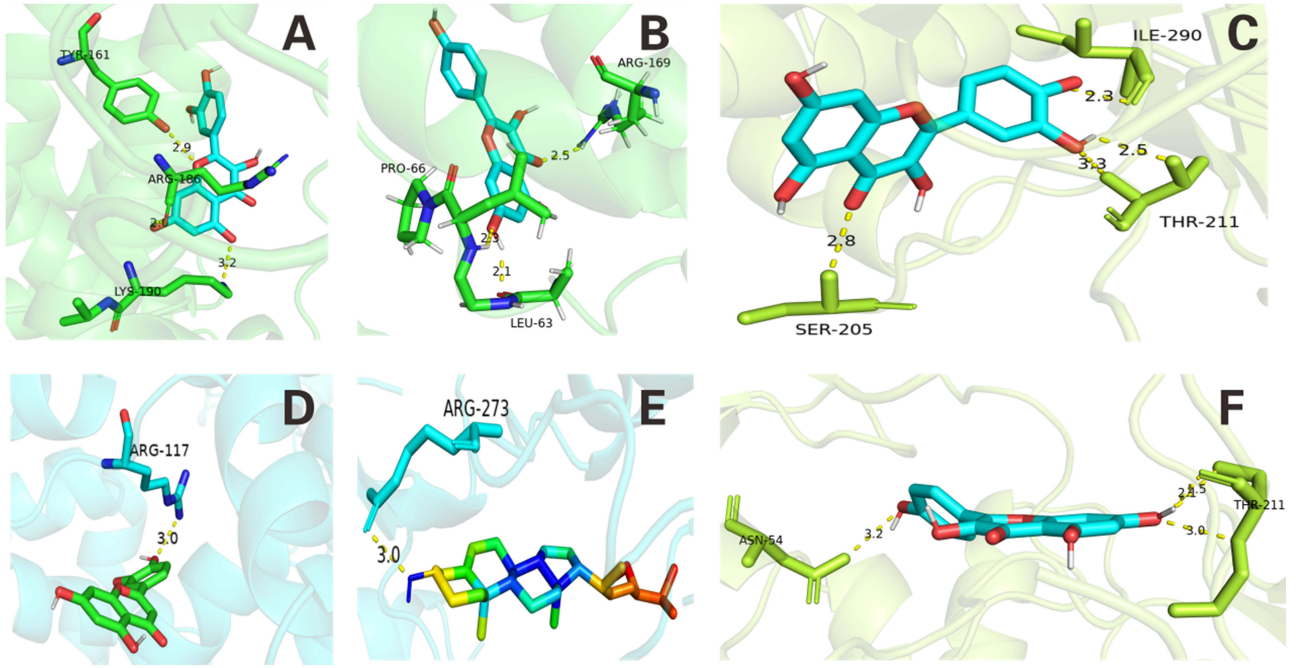

Figure 4 Molecular docking of active ingredients and core protein targets. (**A**–**F**). Molecular docking of SBPD-AECOPD-co-targeted core proteins and active ingredients of SBPD was performed using AutoDock Vina 1.1.2. (**A**). Quercetin-ALB. (**B**). Kaempferol-Interleukin-6. (**C**). Quercetin-Akt1. (**D**). Luteolin-ALB. (**E**). Stigmasterol-Akt1. (**F**). Kaempferol-Akt1.
Abbreviations: SBPD, Sangbaipi decoction; AECOPD, acute exacerbation of chronic obstructive pulmonary disease; ALB, Albumin; Akt1, protein kinase B 1.

Table 2 Binding Energy Between Core Active Ingredients and Core Target Proteins

Name	Code	AKT1	ALB	TNF	IL6	TP53
Quercetin	D1	−9.5	−8.1	−6.6	−7.5	−7.6
beta-Sitosterol	A1	−10.8	−9.2	−6.3	−7.4	−8.0
Kaempferol	E1	−9.1	−8.2	−8.8	−7.4	−7.4
Stigmasterol	F1	−10.9	−9.6	−6.8	−7.2	−8.2
Luteolin	ZSZ6	−9.7	−8.6	−8.9	−7.4	−7.8

with their receptor proteins. This finding preliminarily verified the results of the above network pharmacology analysis as reliable to a certain extent.

SM Improved Lung Function, Histological Abnormalities and Inflammation of Rat Models of AECOPD

To evaluate the therapeutic effect of SM on AECOPD, gavage with SM was carried out in rat models of AECOPD. The induction of AECOPD diminished the total lung and forced vital capacities of rats, concomitant with decreased PIF and PEF (Figure 5A–D, $P < 0.001$). After gavage with SM, rats with AECOPD showed ameliorated pulmonary function, as reflected by enhanced total lung and forced vital capacities and increased PIF and PEF (Figure 5A–D, $P < 0.001$). Further histological examination revealed in the Control group, the structure of the alveolar wall was intact, there was no secretion in the alveolar cavity, no inflammatory cell infiltration, and no widening of the alveolar interval (Figure 5E). However, more chronic inflammatory cells infiltrating around the bronchi, detachment of partial airway mucosal epithelium, compensatory dilation of alveoli, thinning and rupture of the alveolar wall, formation of pulmonary bullae, and dilatation and congestion of septal capillaries in the lung tissues of AECOPD rats (Figure 5E). These pathological changes in the AECOPD rats' lung tissues were mitigated by SM gavage (Figure 5E). In addition, the expressions of IL-6 and TNF-α were increased, while the IL-10 expression were declined in the lung tissues of rats due to the modeling of AECOPD, as shown through qRT-PCR (Figure 5F–H, $P < 0.001$). SM gavage was also found to resist the AECOPD-induced tendencies of the expressions of these inflammatory cytokines in the lung tissues of rats (Figure 5F–H, $P < 0.001$).

SM suppressed lung inflammation and PI3K/Akt signaling activation and restrained systematic inflammation of rat models of AECOPD

Through Western blot, elevated levels of IL-6 and TNF-α and lowered IL-10 levels were detected in the lung tissues of rats following AECOPD induction (Figure 6A–D, $P < 0.05$). AECOPD rats undergoing SM gavage showed lowered IL-6 and TNF-α level and elevated IL-10 level, compared with those without treatment (Figure 6A–D, $P < 0.05$). Furthermore, PI3K/Akt signaling was discovered to be activated in the lung tissues of AECOPD rats, as evidenced by increased expressions of p-PI3K/PI3K and p-Akt/Akt (Figure 6A, E and F, $P < 0.05$), whereas these increases in the expressions of p-PI3K/PI3K and p-Akt/Akt in the lung tissues were offset by SM gavage (Figure 6A, E and F, $P < 0.05$). At the same time, AECOPD rats in contrast with control rats exhibited upregulated serum IL-6 and TNF-α and TGF-β level, while downregulated serum IL-10 levels (Figure 6G–J, $P < 0.01$). SM gavage in AECOPD rats regulated the serum levels of these inflammatory cytokines to change towards the opposite trends (Figure 6G–J, $P < 0.05$).

LY294002 Restored Lung Function and Potentiated the Relieving Effect of SM on Histological Abnormalities of Rat Models of AECOPD

Subsequently, LY294002, an inhibitor of PI3K/AKT signaling, was introduced to investigate how PI3K/AKT signaling is implicated in the effect of SM on AECOPD. Both LY294002 treatment and SM gavage were observed to enhance total lung and forced vital capacities of AECOPD rats, as well as increasing PIF and PEF (Figure 7A–D, $P < 0.001$). However, combined administration of LY294002 treatment and SM gavage revealed an effect similar to the effect exerted by LY294002 treatment

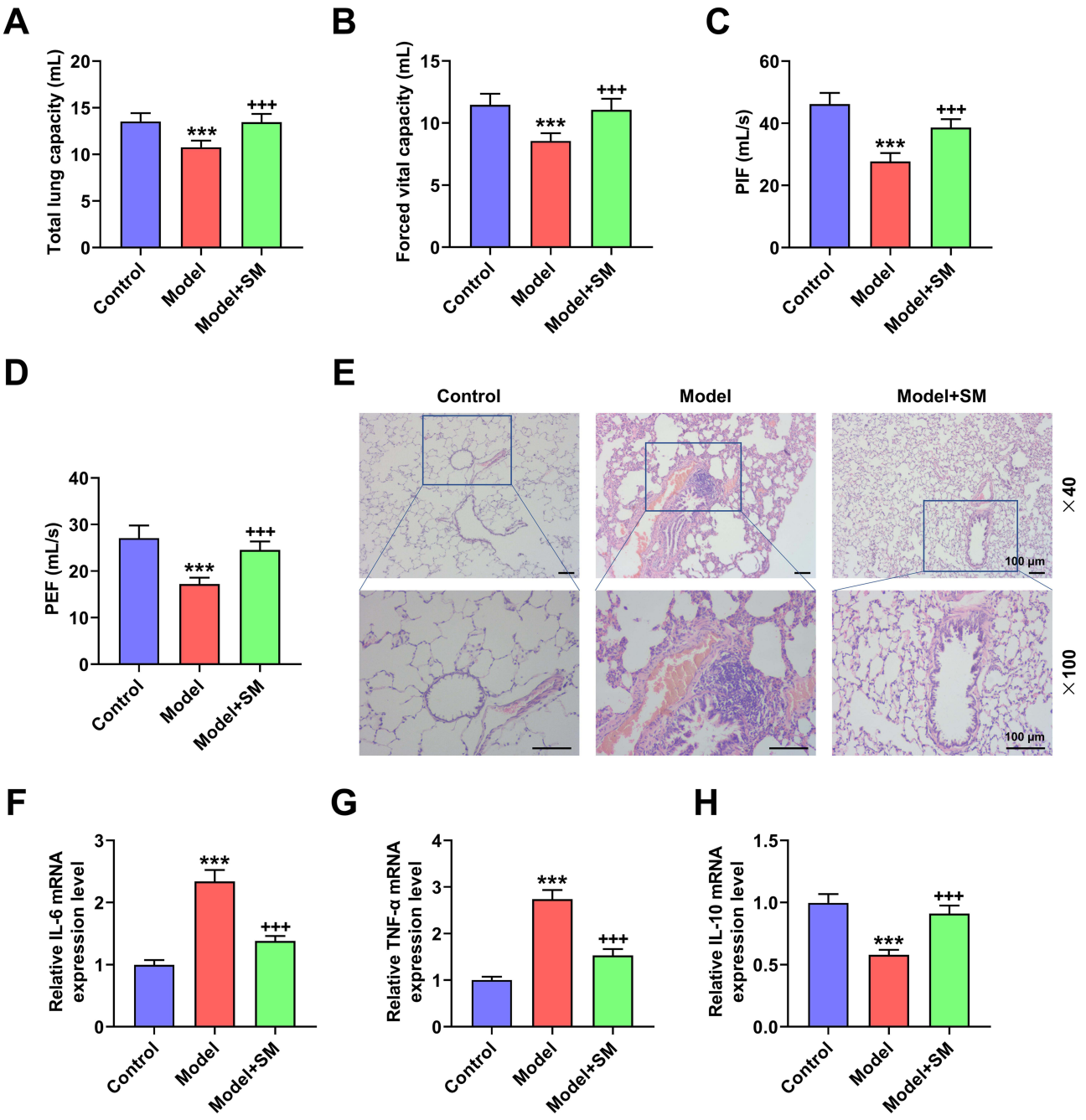

Figure 5 SM improved lung function, histological abnormalities and inflammation of rat models of AECOPD. For inducing AECOPD, male Sprague-Dawley rats were exposed to TS (generated from the combustion of 20 cigarettes) for 30 min twice daily and exposed to aerosolized LPS (1 mg/kg) on the morning of the 7, 14, 21 day. Gavage with SM (200 mg/kg) was conducted after successful modeling. (**A**–**D**). The lung function of rats was assessed utilizing an eSpira Forced Manoeuvers system. (**E**). The lung histopathology of rats was examined via hematoxylin-eosin staining (magnification, ×40/×100; scale, 100 μm). (**F**–**H**). The expressions of IL-6, TNF-α and IL-10 in the lung tissues of rats were assessed by qRT-PCR, with β-actin serving as the normalizer. ***P<0.001 vs Control; ^{+++}P <0.001 vs Model.

Abbreviations: AECOPD, acute exacerbation of chronic obstructive pulmonary disease; SM, stigmasterol; PIF, peak inspiratory flow; PEF, peak expiratory flow; IL-6, interleukin-6; TNF-α, tumor necrosis factor-α; IL-10, interleukin-10; qRT-PCR, quantitative reverse transcription-polymerase chain reaction; TS, tobacco smoke; LPS, lipopolysaccharide.

or by SM gavage alone on the levels of these indexes of AECOPD rats (Figure 7A–D). AECOPD modeling rendered the lung tissues of rats to present promoted inflammatory cell infiltration around the bronchi, detached partial airway mucosal epithelium, compensatively dilated alveoli, thin and ruptured the alveolar wall, pulmonary bulla formation, and dilated and congested septal capillaries (Figure 7E). Alleviation of these pulmonary pathological changes was observed in AECOPD rats

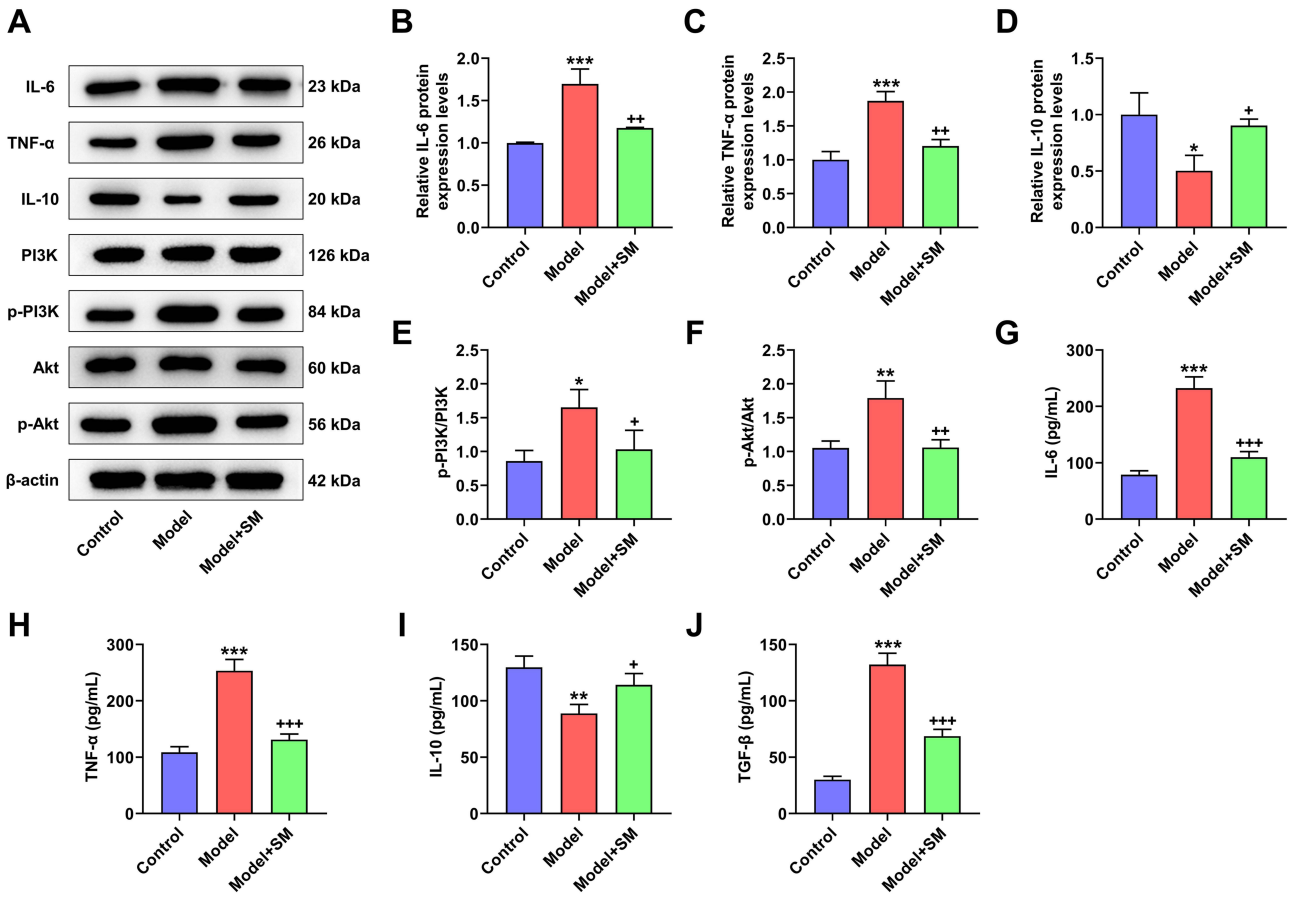

Figure 6 SM suppressed lung inflammation and PI3K/Akt signaling activation and restrained systematic inflammation of rat models of AECOPD. For inducing AECOPD, male Sprague-Dawley rats were exposed to TS (generated from the combustion of 20 cigarettes) for 30 min twice daily and exposed to aerosolized LPS (1 mg/kg) on the morning of the 7, 14, 21 day. Gavage with SM (200 mg/kg) was conducted after successful modeling. (**A**–**F**). The expressions of IL-6, TNF-α, IL-10, p-PI3K/PI3K and p-Akt/Akt in the lung tissues of rats were assessed by Western blot, with β-actin serving as the normalizer. (**G**–**J**). The rat serum levels of IL-6, TNF-α, IL-10 and TGF-β were detected by enzyme-linked immunosorbent assay. **P* <0.05, ***P* <0.01, ****P*<0.001 vs Control; ^{+}P <0.05, ^{++}P <0.01, ^{+++}P <0.001 vs Model.

Abbreviations: AECOPD, acute exacerbation of chronic obstructive pulmonary disease; SM, stigmasterol; IL-6, interleukin-6; TNF-α, tumor necrosis factor-α; IL-10, interleukin-10; TGF-β, transforming growth factor-β; PI3K, phosphoinositide 3-kinase; Akt, protein kinase B; p-PI3K, phosphorated-PI3K; p-Akt, phosphorated-Akt; TS, tobacco smoke; LPS, lipopolysaccharide.

undergoing SM gavage and similar effects were obtained by LY294002 treatment (Figure 7E). Of note, combined administration of LY294002 treatment and SM gavage ameliorated these pulmonary pathological changes induced by AECOPD in rats more potently than LY294002 treatment or SM gavage alone (Figure 7E).

LY294002 augmented the suppressive effect of SM on pulmonary and systematic inflammation of rat models of AECOPD

The expressions of IL-6 and TNF-α along with the p-PI3K/PI3K and p-Akt/Akt expressions declined and the expression of IL-10 soared in the lung tissues of AECOPD rats owing to SM gavage (Figure 8A–F, $P < 0.01$), and LY294002 treatment exerted an effect akin to the effect of SM gavage on the expressions of these inflammatory cytokines (Figure 8A–F, $P < 0.05$). More obvious alterations of these inflammatory cytokines in the lung tissues of AECOPD rats was yielded by combined administration of LY294002 treatment and SM gavage compared with LY294002 treatment alone (Figure 8A–F, $P < 0.05$). Meanwhile, both LY294002 treatment and SM gavage downregulated the serum levels of IL-6, TNF-α and TGF-β, whereas upregulating the IL-10 level in AECOPD rats (Figure 8G–J, P <0.05). Compared with LY294002 treatment alone, LY294002 treatment and SM gavage in combination were more potent in downregulating the serum levels of IL-6, TNF-α and TGF-β (Figure 8G, H and J, $P < 0.05$); yet, combined administration and LY294002 treatment alone had almost similar effects on the serum level of IL-10 (Figure 8I).

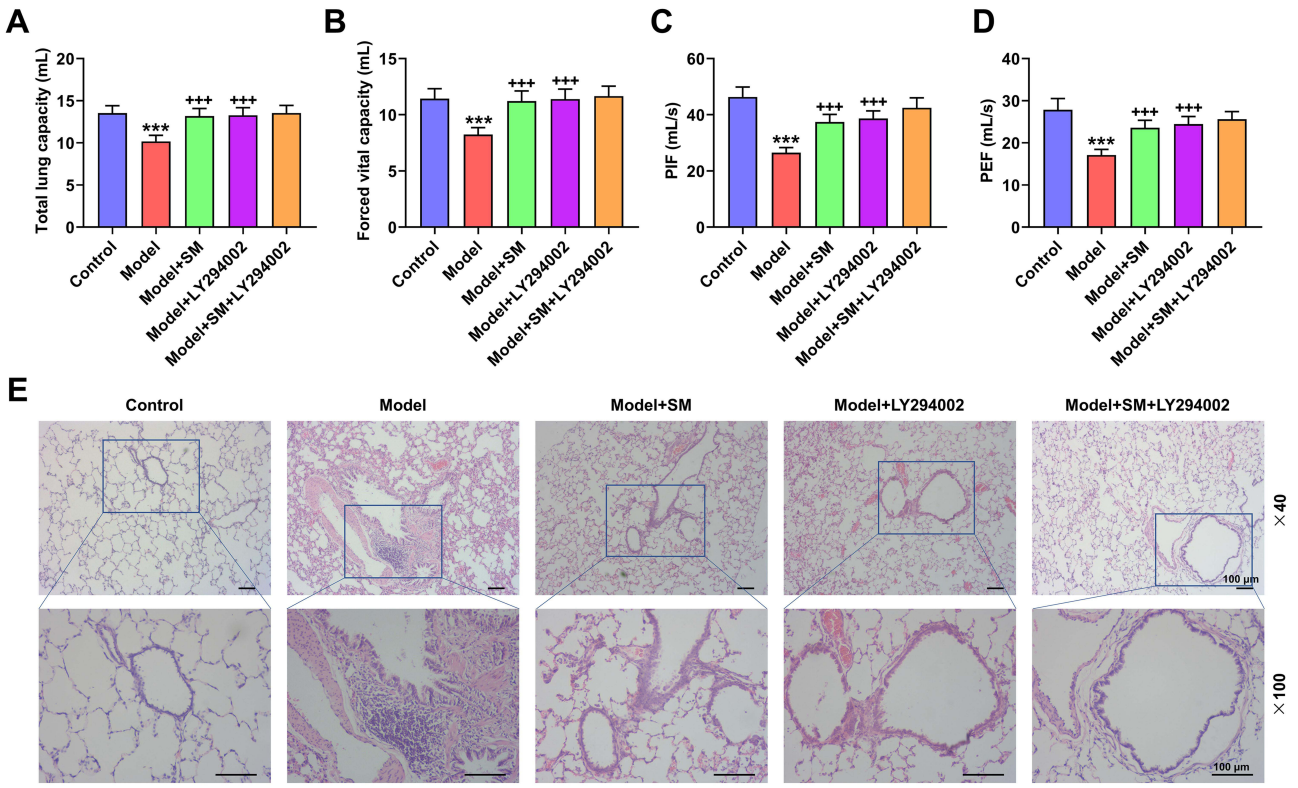

Figure 7 LY294002 restored lung function and potentiated the relieving effect of SM on histological abnormalities of rat models of AECOPD. For inducing AECOPD, male Sprague-Dawley rats were exposed to TS (generated from the combustion of 20 cigarettes) for 30 min twice daily and exposed to aerosolized LPS (1 mg/kg) on the morning of the 7, 14, 21 day. Gavage with SM (200 mg/kg) was conducted after successful modeling. After all the exposure protocols were completed, rats received intraperitoneal injection of an inhibitor of PI3K/Akt, LY294002 (100 μM/kg), once daily. (**A**–**D**). The lung function of rats was assessed utilizing an eSpira Forced Manoeuvers system. (**E**). The lung histopathology of rats was examined via hematoxylin-eosin staining (magnification, ×40/×100; scale, 100 μm). ***P <0.001 vs Control; ^{+++}P <0.001 vs Model.
Abbreviations: AECOPD, acute exacerbation of chronic obstructive pulmonary disease; SM, stigmasterol; PIF, peak inspiratory flow; PEF, peak expiratory flow; TS, tobacco smoke; LPS, lipopolysaccharide.

Discussion

The prevention and relief of AECOPD remain a pivotal goal in the management of COPD[4]. Extensive research has pointed out that reducing disease recurrence is essential to reducing mortality, improving prognosis, preventing complications and elevating the quality of life of patients.[27,28] These underline the significance of increasing the treatment efficiency of AECOPD. SBPD, a traditional Chinese prescription with heat-clearing, phlegm-reducing and anti-inflammatory activities, has shown a significant clinical effect in the treatment of AECOPD, when being combined with Western medicines.[19] Yet, the undefinition of the molecular mechanism of SBPD's action prevents its utilization and promotion in clinical practice. Network pharmacology is a technology that excels at unraveling multi-active ingredient/target/signaling-constituted modules involved in the therapeutic effect of drugs, especially TCM prescriptions with a complex composition.[21,29] Here, our study exploited network pharmacology to provide evidence supporting that SM as one active ingredient of SBPD suppresses PI3K/Akt signaling, thus mitigating AECOPD in rat models.

Network pharmacology has been widely implicated in the clarification of the molecular mechanism of the action of various TCM prescriptions in acute lung injury.[29–31] In these studies, RNA targeted by active ingredients of TCM and differentially expressed genes in diseases were effectively integrated for enriching key targets relevant to the treatment of diseases by TCM prescriptions.[32] With the help of network pharmacological analysis, we obtained 112 active ingredients of SBPD and 277 genes targeted by these active ingredients as well as 5911 AECOPD-relevant genes. Overlapping the two gene target sets yielded 205 targets, which account for 74% of the targets of active ingredients from SBPD, reflecting the reliability and scientificity of SBPD treating AECOPD. Further, PPI construction and analysis resulted in 10 core targets. Through KEGG enrichment analysis, PI3K/Akt signaling was recognized as the signaling pathway critical for

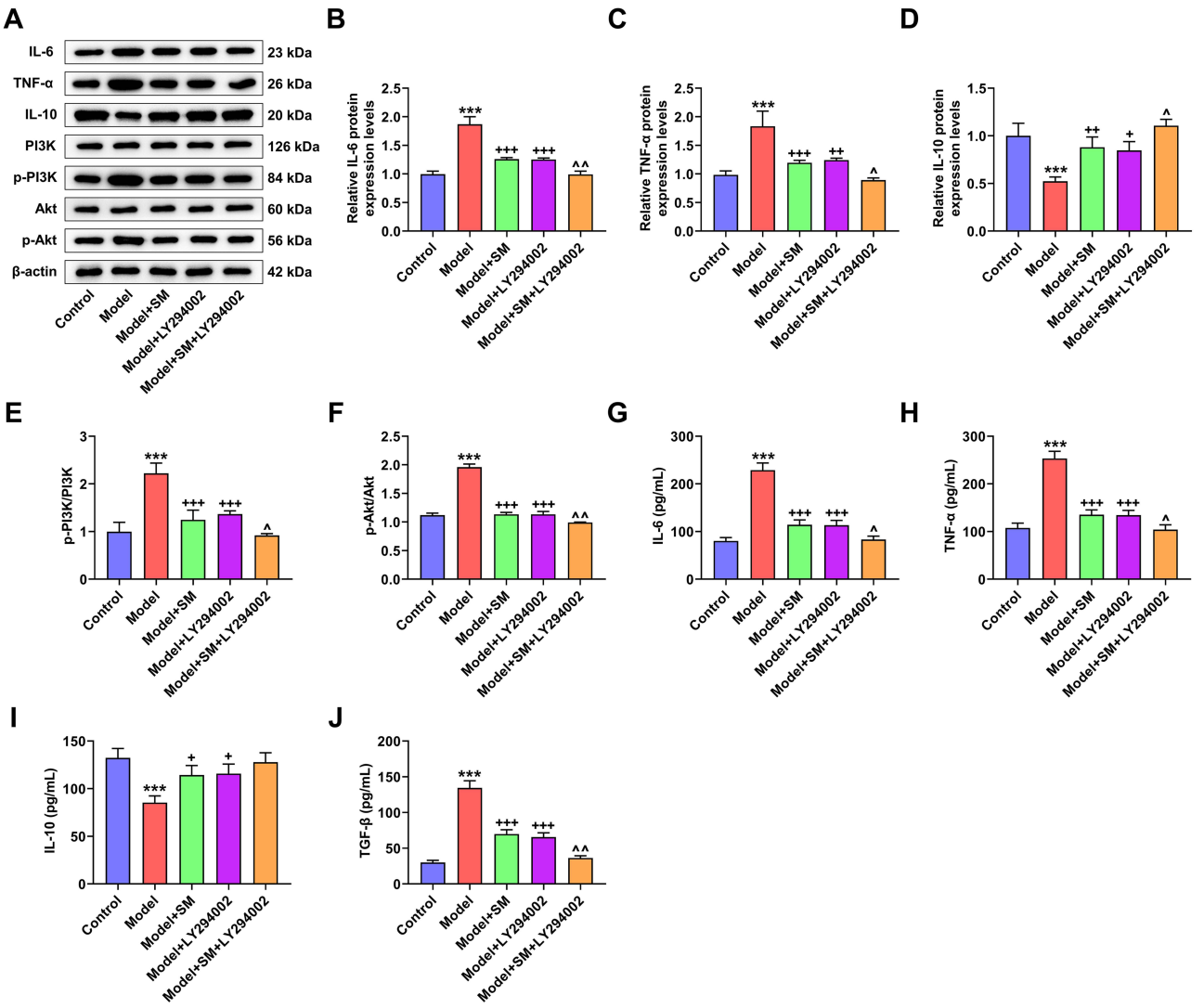

Figure 8 LY294002 augmented the suppressive effect of SM on pulmonary and systematic inflammation of rat models of AECOPD. For inducing AECOPD, male Sprague-Dawley rats were exposed to TS (generated from the combustion of 20 cigarettes) for 30 min twice daily and exposed to aerosolized LPS (1 mg/kg) on the morning of the 7, 14, 21 day. Gavage with SM (200 mg/kg) was conducted after successful modeling. After all the exposure protocols were completed, rats received intraperitoneal injection of an inhibitor of PI3K/Akt, LY294002 (100 μM/kg), once daily. (**A**–**F**). The expressions of IL-6, TNF-α, IL-10, p-PI3K/PI3K and p-Akt/Akt in the lung tissues of rats were assessed by Western blot, with β-actin serving as the normalizer. (**G**–**J**). The rat serum levels of IL-6, TNF-α, IL-10 and TGF-β were detected by enzyme-linked immunosorbent assay. $^{***}P$ <0.001 vs Control; ^{+}P <0.05, ^{++}P <0.01, ^{+++}P <0.001 vs Model; $^{\wedge}P$ <0.05, $^{\wedge\wedge}P$ <0.01 vs Model+LY294002.

Abbreviations: AECOPD, acute exacerbation of chronic obstructive pulmonary disease; SM, stigmasterol; IL-6, interleukin-6; TNF-α, tumor necrosis factor-α; IL-10, interleukin-10; TGF-β, transforming growth factor-β; PI3K, phosphoinositide 3-kinase; Akt, protein kinase B; p-PI3K, phosphorated-PI3K; p-Akt, phosphorated-Akt; TS, tobacco smoke; LPS, lipopolysaccharide.

SBPD to treat AECOPD. Subsequently, from the results of molecular docking simulation, six active ingredient-protein target complexes were derived.

SM is a major phytosterol rich in herbal plants[33] and represents the vital active component, owing to which many TCM prescriptions exert therapeutic effect.[34–36] The pharmacological properties of SM include anti-tumor,[35] anti-inflammatory,[37] anti-oxidative,[34] anti-allergic,[38] and immune-modulatory[39] effects. SM has been proven to exhibit higher conformational stability with ESR1, which is thought to closely relate to the mechanism underlying the treatment of COPD by the Erchen-Xiebai formula.[40] Meanwhile, the SM-Akt1 complex was one of our molecular docking simulation result-derived complexes with a good conformation, and this conformation has been confirmed by previous research and reported to realize anti-ovarian cancer effect by suppressing the PI3K/Akt signaling pathway.[34] These findings combined with our results above demonstrate SM as a molecule of interest with significant importance in the mechanism by which

SBPD alleviates AECOPD, and therefore we chose SM as the research object. Treatment with the Feilike mixture, which contains SM as its key active compositions, ameliorates lung pathological changes of pneumonic rats.[41] Mice with cough variant asthma (CVE) had improved in pulmonary function, histopathology, and the inflammatory state, after being treated with ZhisouSan decoction that contains SM, which has good binding with core targets related to the pathogenesis of CVA.[42] The inhibitory impact of the Erchen-Xiebai formula on COPD is attributed to the binding of SM to COPD-related targets.[40] These above findings hint a role of SM to ameliorate lung dysfunction, histological abnormalities and inflammation. This hint was later verified as reliable in our rat models of AECOPD, based on our results showing gavage with SM ameliorated pulmonary function and histopathology of AECOPD rats, along with inhibited inflammatory response as reflected by downregulated pro-inflammatory IL-6 and TNF-α and upregulated anti-inflammatory IL-10.

Neutrophilic inflammation is a representative mark of COPD and contributes to key pathological features associated with progression to AECOPD.[43] PI3K/Akt signaling is an intracellular signaling pathway which regulates several cellular functions and plays a vital role in the induction of pulmonary inflammation through reducing neutrophil apoptosis.[44] Its activation leads to activation of the mechanistic target of rapamycin, an important serine threonine protease, thereby increasing the pulmonary inflammatory injuries, such as airway inflammation, barrier disruption and pulmonary edema.[45,46] PI3K/Akt signaling has been proven to be activated and mediate systematic inflammation in COPD.[47] Suppression of PI3K/Akt signaling restricts airway mucus hypersecretion in airway of AECOPD.[48] Our study detected that SM gavage suppressed PI3K/Akt signaling activation in the lung tissues of AECOPD rats. In AECOPD, the inflammatory burst in the airways emerges as the primary inflammatory event, which can culminate in systemic manifestations, as indicated by elevation of blood inflammatory proteins or cytokines.[6] Since PI3K/Akt signaling activation is linked to systematic inflammation in COPD, we surmised that the suppression of PI3K/Akt signaling by SM might come with dampened systematic inflammatory responses, which was later confirmed as authentic by our detection of inflammatory cytokines in serum samples.

Moreover, the activation of PI3K/Akt signaling initiates the process of angiogenesis, with elevated levels of direct/indirect proangiogenic makers, like vascular endothelial growth factor and TGF-β, which contributes to migration and proliferation of endothelial cells in existing vessels to induce neovascularization and thus cause lung disorder.[49] TGF-β is a multi-functional cytokine acting as a proinflammatory protein and also an indirect proangiogenic maker that activates signal transduction and activator of transcription 3, thereby upregulating of angiogenic mediator and leading to angiogenesis.[49] Besides, TGF-β activation is a mechanism central to pulmonary fibrosis,[50] a pathological event that may occur in COPD patients. In our study, AECOPD rats undergoing SM gavage showed a subdued serum level of TGF-β, which was accompanied by suppressed PI3K/Akt signaling. The above findings and results together accentuate the importance of the suppression of PI3K/Akt signaling by SM in the treatment of AECOPD.

To ascertain whether the alleviating effect of SM on AECOPD is attributed to the suppression of PI3K/Akt signaling, injection of LY294002 was applied to AECOPD rats receiving SM gavage. Our *in-vivo* data validated that it is due to the suppression of PI3K/Akt signaling that SM is able to deliver significant protection against AECOPD-associated lung injury. However, there are some limitation in this study. Firstly, the optimal dose and concentration of SM was not explored in vivo or in vitro; secondly, the safety of the SM was not evaluated; thirdly, Sangbaipi decoction administration group was not design in this study to further verified the experimental results.

Conclusion

In conclusion, by utilizing systematic network pharmacology, our present study unveiled that SM as an active component of SBPD targets PI3K/Akt signaling to reduce pulmonary dysfunction, relieve pulmonary histological abnormalities and dampen systematic inflammation in rat models of AECOPD, which gives insights into the pharmacological mechanisms underlying the treatment by SBPD for AECOPD and benefits the clinical application and promotion of SBPD.

Funding

This work was supported by the 2023 Zhejiang TCM Science and Technology Plan [2023ZR074].

Disclosure

The authors declare no conflicts of interest in this work.

References

1. Labaki WW, Rosenberg SR. Chronic Obstructive Pulmonary Disease. *Ann Internal Med*. 2020;173(3):Itc17–itc32. doi:10.7326/AITC202008040
2. Ferrera MC, Labaki WW, Han MK. Advances in Chronic Obstructive Pulmonary Disease. *Ann Rev Med*. 2021;72(1):119–134. doi:10.1146/annurev-med-080919-112707
3. Yingqiao L, Dandan W, Lingling G, Wendan W. Evaluation of Treatment Efficacy and Safety of ACBT in Patients with Chronic Obstructive Pulmonary Disease: a Systematic Review and Meta-Analysis. *J Biol Regul Homeost Agents*. 2023;37(6):3363–3373.
4. Ritchie AI, Wedzicha JA. Definition Causes, Pathogenesis, and Consequences of Chronic Obstructive Pulmonary Disease Exacerbations. *Clinics Chest Med*. 2020;41(3):421–438. doi:10.1016/j.ccm.2020.06.007
5. Vogelmeier CF, Román-Rodríguez M, Singh D, Han MK, Rodríguez-Roisin R, Ferguson GT. Goals of COPD treatment: focus on symptoms and exacerbations. *Respir Med*. 2020;166:105938. doi:10.1016/j.rmed.2020.105938
6. MacLeod M, Papi A, Contoli M, et al. Chronic obstructive pulmonary disease exacerbation fundamentals: diagnosis, treatment, prevention and disease impact. *Respirology*. 2021;26(6):532–551. doi:10.1111/resp.14041
7. Halpin DMG, Criner GJ, Papi A, et al. Global Initiative for the Diagnosis, Management, and Prevention of Chronic Obstructive Lung Disease. The 2020 GOLD Science Committee Report on COVID-19 and Chronic Obstructive Pulmonary Disease. *Am J Respir Crit Care Med*. 2021;203(1):24–36. doi:10.1164/rccm.202009-3533SO
8. Kunadharaju R, Sethi S. Treatment of Acute Exacerbations in Chronic Obstructive Pulmonary Disease. *Clinics Chest Med*. 2020;41(3):439–451. doi:10.1016/j.ccm.2020.06.008
9. Wang Y, Wang YJG, Medicine So C. Analysis of the development course of traditional Chinese medicine standardization and recommendations on future work. *Guidelines and Standards of Chinese Medicine*. 2023;1(1):1–8. doi:10.1097/gscm.0000000000000009
10. Zhang S-Q, Jiang -X-X, J-C L. Traditional Chinese medicine in human diseases treatment: new insights of their potential mechanisms. *Anat Record*. 2023;306(12):2920–2926. doi:10.1002/ar.25228
11. Wang R, Wang Y, Fang L, et al. Efficacy and safety of traditional Chinese medicine in the treatment of menopause-like syndrome for breast cancer survivors: a systematic review and meta-analysis. *BMC Cancer*. 2024;24(1):42. doi:10.1186/s12885-023-11789-z
12. Chan HHL, Ng T. Traditional Chinese Medicine (TCM) and Allergic Diseases. *Current Allergy and Asthma Rep*. 2020;20(11):67. doi:10.1007/s11882-020-00959-9
13. Gao J, Hou T. Cardiovascular disease treatment using traditional Chinese medicine:Mitochondria as the Achilles' heel. *Biomed Pharmacothe*. 2023;164:114999. doi:10.1016/j.biopha.2023.114999
14. Xu F, Zhang H, Chen J, et al. Recent progress on the application of compound formulas of traditional Chinese medicine in clinical trials and basic research in vivo for chronic liver disease. *J Ethnopharmacol*. 2024;321:117514. doi:10.1016/j.jep.2023.117514
15. Wei Z, Chen J, Zuo F, et al. Traditional Chinese Medicine has great potential as candidate drugs for lung cancer: a review. *J Ethnopharmacol*. 2023;300:115748. doi:10.1016/j.jep.2022.115748
16. Chen R, Zhang L, Gu W, et al. Lung function benefits of traditional Chinese medicine Qiju granules against fine particulate air pollution exposure: a randomized controlled trial. *Front Med*. 2024;11:1370657. doi:10.3389/fmed.2024.1370657
17. Zhang C, Yang H, Gan W, et al. A randomized controlled trial for prevention of acute exacerbation of stable chronic obstructive pulmonary disease with acupoint application of traditional Chinese medicine: study protocol clinical trial (SPIRIT Compliant). *Medicine*. 2020;99(10):e19396. doi:10.1097/MD.0000000000019396
18. Zhen G, Jing J, Fengsen L. Traditional Chinese medicine classic herbal formula Xiaoqinglong decoction for acute exacerbation of chronic obstructive pulmonary disease: a systematic review protocol. *Medicine*. 2018;97(52):e13761. doi:10.1097/MD.0000000000013761
19. Liu S, Chen J, Zuo J, Lai J, Wu L, Guo X. Comparative effectiveness of six Chinese herb formulas for acute exacerbation of chronic obstructive pulmonary disease: a systematic review and network meta-analysis. *BMC Complementary and Alternative Medicine*. 2019;19(1):226. doi:10.1186/s12906-019-2633-2
20. Li J, Jiang J, Jing C, Zheng W, Pan H. Efficacy and safety of Sangbaipi Decoction in patients with acute exacerbation of chronic obstructive pulmonary disease: a protocol for systematic review and meta analysis. *Medicine*. 2020;99(44):e22917. doi:10.1097/MD.0000000000022917
21. Nogales C, Mamdouh ZM, List M, Kiel C, Casas AI, Schmidt H. Network pharmacology: curing causal mechanisms instead of treating symptoms. *Trends Pharmacol Sci*. 2022;43(2):136–150. doi:10.1016/j.tips.2021.11.004
22. Li X, Wei S, Niu S, et al. Network pharmacology prediction and molecular docking-based strategy to explore the potential mechanism of Huanglian Jiedu Decoction against sepsis. *Comput Biol Med*. 2022;144:105389. doi:10.1016/j.compbiomed.2022.105389
23. Liao X, Yijing Z, Hongmei T, et al. Improvement Effects of Weijing Decoction on AECOPD Model Rats and Its Mechanism. *China Pharm*. 2021;32(21):2593–2598.
24. Poulose N, Sajayan A, Ravindran A, et al. Anti-diabetic Potential of a Stigmasterol From the Seaweed Gelidium spinosum and Its Application in the Formulation of Nanoemulsion Conjugate for the Development of Functional Biscuits. *Frontiers in Nutrition*. 2021;8:694362. doi:10.3389/fnut.2021.694362
25. Jia M, Qiu H, Lin L, Zhang S, Li D, Jin D. Inhibition of PI3K/AKT/mTOR Signalling Pathway Activates Autophagy and Suppresses Peritoneal Fibrosis in the Process of Peritoneal Dialysis. *Front Physiol*. 2022;13:778479. doi:10.3389/fphys.2022.778479
26. Livak KJ, Schmittgen TD. Analysis of relative gene expression data using real-time quantitative PCR and the $2^{-\Delta\Delta C}{}_{T}$ Method. *Methods San Diego Calif*. 2001;25(4):402–408. doi:10.1006/meth.2001.1262
27. Chen X, Gong D, Huang H, Wang K, Zhang W, Li S. Expert consensus and operational guidelines on exercise rehabilitation of chronic obstructive pulmonary disease with integrating traditional Chinese medicine and Western medicine. *J Thoracic Dis*. 2021;13(6):3323–3346. doi:10.21037/jtd-21-431
28. Baqdunes MW, Leap J, Young M, Kaura A, Cheema T. Acute Exacerbation of Chronic Obstructive Pulmonary Disease. *Critical Care Nurs Quart*. 2021;44(1):74–90. doi:10.1097/CNQ.0000000000000341

29. Wang Y, Yuan Y, Wang W, et al. Mechanisms underlying the therapeutic effects of Qingfeiyin in treating acute lung injury based on GEO datasets, network pharmacology and molecular docking. *Comput Biol Med*. 2022;145:105454. doi:10.1016/j.compbiomed.2022.105454
30. Zhu H, Wang S, Shan C, et al. Mechanism of protective effect of xuan-bai-cheng-qi decoction on LPS-induced acute lung injury based on an integrated network pharmacology and RNA-sequencing approach. *Respir Res*. 2021;22(1):188. doi:10.1186/s12931-021-01781-1
31. Ding Z, Zhong R, Yang Y, et al. Systems pharmacology reveals the mechanism of activity of Ge-Gen-Qin-Lian decoction against LPS-induced acute lung injury: a novel strategy for exploring active components and effective mechanism of TCM formulae. *Pharmacol Res*. 2020;156:104759. doi:10.1016/j.phrs.2020.104759
32. Liu C, Yin Z, Feng T, Zhang M, Zhou Z, Zhou Y. An integrated network pharmacology and RNA-Seq approach for exploring the preventive effect of Lonicerae japonicae flos on LPS-induced acute lung injury. *J Ethnopharmacol*. 2021;264:113364. doi:10.1016/j.jep.2020.113364
33. Woyengo TA, Ramprasath VR, Jones PJ. Anticancer effects of phytosterols. *Eur J Clin Nutr*. 2009;63(7):813–820. doi:10.1038/ejcn.2009.29
34. Mo Z, Xu P, Li H. Stigmasterol alleviates interleukin-1beta-induced chondrocyte injury by down-regulating sterol regulatory element binding transcription factor 2 to regulateferroptosis. *Bioengineered*. 2021;12(2):9332–9340. doi:10.1080/21655979.2021.2000742
35. Chen Z, Lin T, Liao X, et al. Network pharmacology based research into the effect and mechanism of Yinchenhao Decoction against Cholangiocarcinoma. *ChinMed*. 2021;16(1):13. doi:10.1186/s13020-021-00423-4
36. Li JX, Han ZX, Cheng X, et al. Combinational study with network pharmacology, molecular docking and preliminary experiments on exploring common mechanisms underlying the effects of weijing decoction on various pulmonary diseases. *Heliyon*. 2023;9(5):e15631. doi:10.1016/j.heliyon.2023.e15631
37. Jie F, Yang X, Yang B, Liu Y, Wu L, Lu B. Stigmasterol attenuates inflammatory response of microglia via NF-κB and NLRP3 signaling by AMPK activation. *Biomed Pharmacothe*. 2022;153:113317. doi:10.1016/j.biopha.2022.113317
38. Antwi AO, Obiri DD, Osafo N, Essel LB, Forkuo AD, Atobiga C. Stigmasterol Alleviates Cutaneous Allergic Responses in Rodents. *Biomed Res Int*. 2018;2018:3984068. doi:10.1155/2018/3984068
39. Bouic PJ. The role of phytosterols and phytosterolins in immune modulation: a review of the past 10 years. *Curr Opin Clin Nutr Metab Care*. 2001;4(6):471–475. doi:10.1097/00075197-200111000-00001
40. Ye H, He B, Zhang Y, et al. Herb-symptom analysis of Erchen decoction combined with Xiebai powder formula and its mechanism in the treatment of chronic obstructive pulmonary disease. *Front Pharmacol*. 2023;14:1117238. doi:10.3389/fphar.2023.1117238
41. Peng J, Chen X, Hou M, et al. The TCM Preparation Feilike Mixture for the Treatment of Pneumonia: network Analysis, Pharmacological Assessment and Silico Simulation. *Front Pharmacol*. 2022;13:794405. doi:10.3389/fphar.2022.794405
42. Guo DH, Hao JP, Li XJ, Miao Q, Zhang Q. Exploration in the Mechanism of Zhisou San for the Treatment of Cough Variant Asthma Based on Network Pharmacology. *Evidence-Base Com Alter Med*. 2022;2022:1698571. doi:10.1155/2022/1698571
43. Jasper AE, McIver WJ, Sapey E, Walton GM. Understanding the role of neutrophils in chronic inflammatory airway disease. *F1000Research*. 2019;8:8. doi:10.12688/f1000research.17047.1
44. Zhao H, Ma Y, Zhang L. Low-molecular-mass hyaluronan induces pulmonary inflammation by up-regulation of Mcl-1 to inhibit neutrophil apoptosis via PI3K/Akt1 pathway. *Immunology*. 2018;155(3):387–395. doi:10.1111/imm.12981
45. Hsieh YH, Deng JS, Chang YS, Huang GJ. Ginsenoside Rh2 Ameliorates Lipopolysaccharide-Induced Acute Lung Injury by Regulating the TLR4/PI3K/Akt/mTOR, Raf-1/MEK/ERK, and Keap1/Nrf2/HO-1 Signaling Pathways in Mice. *Nutrients*. 2018;10(9):1208. doi:10.3390/nu10091208
46. Hu Y, Lou J, Mao YY, et al. Activation of MTOR in pulmonary epithelium promotes LPS-induced acute lung injury. *Autophagy*. 2016;12(12):2286–2299. doi:10.1080/15548627.2016.1230584
47. Sun X, Chen L, He Z. PI3K/Akt-Nrf2 and Anti-Inflammation Effect of Macrolides in Chronic Obstructive Pulmonary Disease. *Current Drug Meta*. 2019;20(4):301–304. doi:10.2174/1389200220666190227224748
48. Feng F, Du J, Meng Y, Guo F, Feng C. Louqin Zhisou Decoction Inhibits Mucus Hypersecretion for Acute Exacerbation of Chronic Obstructive Pulmonary Disease Rats by Suppressing EGFR-PI3K-AKT Signaling Pathway and Restoring Th17/Treg Balance. *Evidence-Based Comp Alterna Med*. 2019;2019:6471815.
49. Laddha AP, Kulkarni YA. VEGF and FGF-2: promising targets for the treatment of respiratory disorders. *Respir Med*. 2019;156:33–46. doi:10.1016/j.rmed.2019.08.003
50. Chanda D, Otoupalova E, Smith SR, Volckaert T, De Langhe SP, Thannickal VJ. Developmental pathways in the pathogenesis of lung fibrosis. *Mol Aspect Med*. 2019;65:56–69. doi:10.1016/j.mam.2018.08.004